A review of the genus *Pseudoromicia* (Chiroptera: Vespertilionidae), with a description of a new species

Amanda L. Grunwald[1], Terrence C. Demos[2], Yvette Nguéagni[3], Martin N. Tchamba[3], Ara Monadjem[5,6], Paul W. Webala[4], Julian C. Kerbis Peterhans[2], Bruce D. Patterson[2], and Luis A. Ruedas[1]

[1]Department of Biology and Museum of Vertebrate Biology, Portland State University, SRTC–247, P. O. Box 751, Portland, Oregon 97207

[2]Negaunee Integrative Research Center, Field Museum of Natural History, Chicago, Illinois 60605

[3]Department of Forestry, Faculty of Agronomy and Agricultural Sciences, University of Dschang, Cameroon

[4]Department of Forestry and Wildlife Management, Maasai Mara University, P.O. Box 861, Narok 20500, Kenya

[5]Department of Biological Sciences, University of Eswatini, Private Bag 4, Kwaluseni, Eswatini

[6]Mammal Research Institute, Department of Zoology & Entomology, University of Pretoria, Private Bag 20, Hatfield 0028, Pretoria, South Africa

ABSTRACT

The Cameroon Volcanic Line, which divides the Congo Basin fauna from the West African fauna, is a known area of high endemism for various taxa, but the region's bat fauna has received little attention. We review variation in morphological and molecular (mitochondrial

Cytochrome *b*) characters in the Tropical African vespertilionid bat genus *Pseudoromicia*. Assessment of this variation indicates the existence of a new species of *Pseudoromicia*, from the Mbam Minkom Massif in the Centre Region of Cameroon. The new species is diagnosable by sequence data and is morphologically similar to its putative sister taxon, *P. kityoi*, from Uganda. Although we suggest that it be assigned to the IUCN category of Data Deficient, there should be some concern as to the conservation status of this species: the Mbam Minkom Massif ecosystem is threatened due to lack of legal conservation frameworks and exposure to increasing human pressure. The new species is in a clade with *P. roseveari* and *P. kityoi*. These three species may be relicts of a single widespread species originating in the West African "white-winged" group of *Pseudoromicia* that then spread east across the tropical moist broadleaf forest into East Africa, and are now restricted to a few upland rainforest patches in West Africa (*P. roseveari*), in outliers of the Cameroon Volcanic Line region (*Pseudoromicia* sp.), and the Lake Victoria area (*P. kityoi*). The smaller, white-winged species are hypothesized to be ancestral, with one extant putative species (*P. rendalli*) also extending into East and southern Africa (Van Cakenberghe & Happold, 2013). The larger, dark-winged taxa likely dispersed to East Africa and subsequently back to West Africa (e.g., *Pseudoromicia* sp., *P. roseveari*). Our data illustrate the potential importance of the Dahomey Gap and climatic changes in the evolution of this group of species.

Keywords: Africa, Cameroon, bat, mitochondrial DNA, systematics, taxonomy

INTRODUCTION

The taxonomy and systematic relationships among pipistrelle-like bats of the tribe Vespertilionini continue to remain poorly known; this void in knowledge is well exemplified in Africa (Monadjem, Richards, et al., 2021). Previous analyses of African pipistrelle-like bats have documented genetic diversity but more modest morphological differentiation that have resulted in unstable taxonomic arrangements and poorly understood systematic relationships. These unresolved relationships have obscured true bat diversity in many regions (Decher et al., 2015; Hutterer et al., 2019; Monadjem et al., 2020). Recent work by Monadjem, Richards, et al. (2021), Monadjem, Demos, et al. (2021), reviewing nearly all the known sub-Saharan pipistrelle-like bats in the tribes Vespertilionini and Pipistrellini, elucidated the systematic relationships of many bat clades within these tribes. These works revealed five distinct genera previously contained within *Neoromicia*. African Vespertilionini currently are hypothesized to include the expanded genera *Laephotis* and *Nycticeinops*, a restricted *Neoromicia*, and the newly described *Pseudoromicia* and *Afronycteris* (Monadjem, Demos, et al., 2021).

Species in the newly recognized genus *Pseudoromicia* are distributed widely across sub-Saharan Africa, with the majority occurring within the African Equatorial belt, and particularly associated with African tropical forests. They have a preference for forest edges (Monadjem, Demos, et al., 2021), although a single species, *Pseudoromicia rendalli*, also occurs in wetlands near forested habitats, as well as extending far into savanna habitats (Monadjem, Demos, et al., 2021). Diversity within this group seems to be highest in the Guinea forest zone of West Africa, where four species were identified in a single forest patch (Monadjem et al., 2016; Monadjem, Demos, et al., 2021). The genus contains both white-winged and dark-winged forms, with

molecular studies suggesting white-winged species may be ancestral for *Pseudoromicia* (Monadjem, Demos, et al., 2021).

As currently understood (Juste et al., 2023; Monadjem, Demos, et al., 2021), *Pseudoromicia* is hypothesized to contain nine species: *P. brunnea* (Thomas, 1880), *P. isabella* (Decher, Hutterer, & Monadjem et al., 2016 [in Decher et al., 2015]), *P. kityoi* (Monadjem, Kerbis, Peterhans, Nalikka, Waswa, Demos, & Patterson, 2021 [in Monadjem, Richards, et al., 2021])), *P. nyanza* (Monadjem, Patterson, Webala, & Demos, 2021 [in Monadjem, Richards, et al., 2021])), *P. rendalli* (Thomas, 1889), *P. roseveari* ((Monadjem, Richards, Taylor, & Stoffberg, 2013)), *P. tenuipinnis* (Peters, 1872), an undescribed species from Tanzania (Monadjem, Demos, et al., 2021), and a newly described oceanic island species, *P.* sp., from Principe Isl. (Juste et al., 2023). Here, we describe an upland bat species from a singular mountainous formation in Cameroon, the Mbam Minkom Massif, located in the extreme north-western extent of the North-western Congolian Lowland Forest ecoregion (*sensu* Olson et al., 2001), and about 190 km to the south-east of the Cameroon Volcanic Line as delineated by Denys et al. (2014), which is known to harbour a high diversity of mammalian endemics (Eisentraut, 1973). With the addition of this new species from Cameroon, *Pseudoromica* comes to include 10 species.

The Mbam Minkom Massif is an unprotected ecosystem, and its bat diversity is poorly known. Likewise, bat distribution and diversity across Cameroon largely remains undiscovered: historically, few surveys have been undertaken there by bat researchers, with the notable exceptions of Aellen (1952), Perret and Aellen (1956), and Eisentraut (1941, 1956, 1957, 1963, 1973), although some valuable regional surveys also have been carried out (e.g., Fedden & MacLeod, 1986). Recent studies by Bakwo Fils and co-workers are revealing Cameroon's

exceptional bat diversity (Bakwo Fils et al., 2014, Dongmo et al., 2020; Lebreton et al., 2014; Manga Mongombe et al., 2019; Waghiiwimbom et al., 2020). Notwithstanding, large gaps still remain and more field data are necessary (Waghiiwimbom et al., 2020) because bat species from Cameroon rarely are considered in long-term conservation plans (Bakwo Fils, 2010).

MATERIALS AND METHODS

Study site.— The present study is based on a collection of bats (Mammalia: Chiroptera) captured in August 2019 across four sites in the Mbam Minkom Massif (Fig. 1), an isolated inselberg located near Yaoundé, in the Lekié Department of Centre Province, Cameroon. The collection included 51 specimens of 18 species in five families and will be described in more detail in a separate work. Cameroon's Mbam Minkom Massif (MMM), centred at ca. 3°57.73′N, 11°23.50′E, is a ~4500 ha isolated gneiss inselberg with a fragment of submontane forest remaining on it (Bissaya et al., 2018). The massif is located near the intersection of four distinct ecoregions: the above mentioned Congolian, Atlantic Equatorial Coastal Forest, cross–Sanaga–Bioko Coastal Forest, and northern Congolian Forest–Savanna Mosaic (Linder et al., 2012; Olson et al., 2001). All ecoregions are part of the Guineo–Congolian phytogeographic centre of endemism as described by White (1983). Ranging in elevation from surrounding plains at 650 m to its 1295 m summit, the Mbam Minkom range is topographically diverse, consisting of steep, rugged, hilly terrain with steep-sided valleys and broad ridge tops. Mt Mbam Minkom (1295 m) is the highest peak in the range, which also includes: Mt Odou (1225 m), Mt Nkolakie (1185 m), Mt Nkoldjobe (1181 m), Mt Nkoloman (1060 m), Mt Ekondongo (1171 m), Mt Miviami Zibin (1141 m), Mt Zoabissima (1120 m), and Mt Mbikal (1221 m).

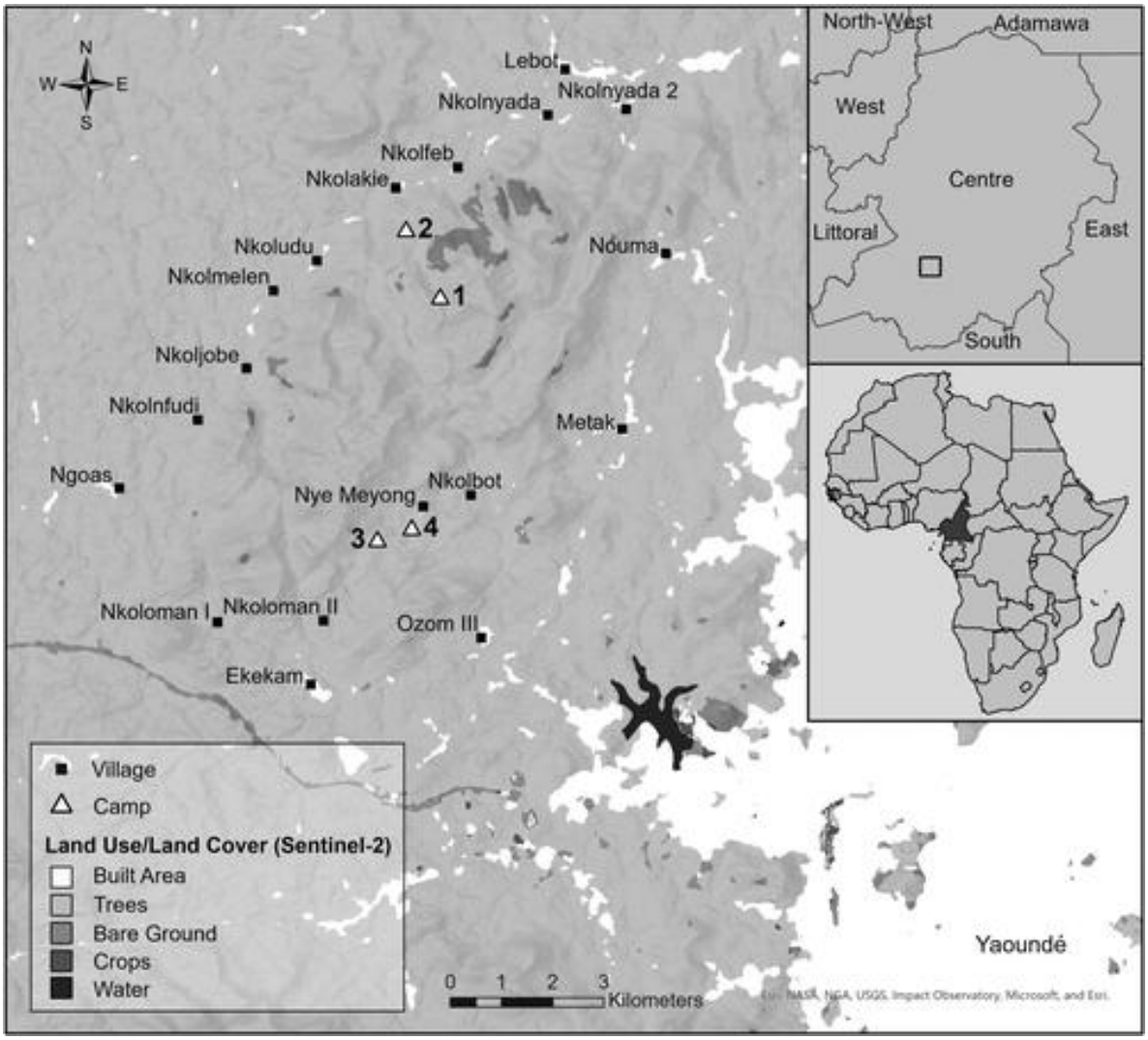

Figure 1. Land cover map showing collecting camps and villages surrounding the Mbam Minkom Massif, Lekié Department, Centre Province, Cameroon. Coordinates (Datum: WGS84) of each collecting camps are as follows, Camp 1: 3°57.481′ N, 11°22.999′ E, 1074 m; Camp 2: 3°58.156′ N, 11°22.840′E, 785 m; Camp 3: 3°55.006′ N, 11°22.400′ E, 884 m; Camp 4: 3°55.072′ N, 11°22.639′ E, 829 m. Inset (upper): location of Mbam Minkom Massif within Cameroon's Centre Region; Inset (lower): location of Cameroon within Africa. Map created using ArcGIS software by Esri (2020) including datasets from: USGS, land use/land cover data from ESA's Sentinel-2 produced by Esri, Microsoft, and Impact Observatory (2021); village location from Awa et al. (2009).

Specimens examined.— During the evening of 14 August 2019, we captured a pipistrelle-like bat on Mt Mbam Minkom. The bat was captured at our second camp, situated at 785 m (Fig. 1), on

the north-west slope of Mt Mbam Minkom, adjacent to the Bitemgu River. Four mist nets (30 mm mesh, 70 denier, 2-ply, 2.6 m high by 6 m long) were set across the river ~3 m apart. Two additional nets (30 mm mesh, 70 denier, 2-ply, 2.6 m high by 12 m long) were set downstream, flanking an area where the river pooled. Both of these latter nets were set parallel to the stream, running perpendicular to forest openings on either side. Nets were opened before dusk (about 18:00) and closed at 01:00 hours then reopened at 04:00 hours and closed at sunrise.

This bat was caught in a net set across the Bitemgu river between 18:00 and 21:00 hours. Collection followed established methods (Ferreira et al., 2021; Flaquer et al., 2007) and best practices (Sikes et al., 2016), and was approved by the Portland State University Institutional Animal Care and Use Committee (Protocol #74). After euthanasia, the bat was field-catalogued and measured. External measurements in millimetres (to 1.0 mm) were taken with a steel ruler using standard notation and included: total length (head and body plus tail), tail length, hindfoot length (including claw), ear pinna length from notch, and tragus length. Body mass was recorded to the nearest 0.5 g using a Pesola spring scale (Pesola Präzisionswaagen AG, Schindellegi, Switzerland). The skull was extracted carefully in the laboratory such that the morphology of the ears, lips, and nose still remained apparent and could be studied. The skull and mandible subsequently were cleaned by dermestid beetles for study (Hall & Russell, 1933; Pahl, 2020; Russell, 1947). Wing bone measurements were recorded in the laboratory with a digital caliper at 0.01 mm accuracy (). Specimens used in interspecific comparisons are listed in Supplemental Appendix 1.

Table 4.— Wing measurements of the holotype ofPseudoromicia mbamminkomsp. nov. Measured wingvariables include: metacarpals (mt) and phalanx (ph).

Wing bone	Measurement (mm)
2mt	33.30
3mt	34.72
1ph3mt	12.92
2ph3mt	17.05
4mt	34.39
1ph4mt	11.37
2ph4mt	9.39
5mt	33.13
1ph5mt	7.80
2ph5mt	5.18

Univariate morphological analyses.— Eleven cranial and four dental measurements were taken with caliper to the closest 0.01 mm, following Velazco and Gardner (2012). Mensural variables (Fig. 2) included: greatest length of skull (GLS); condyloincisive length (CIL); condylocanine length (CCL); zygomatic breadth (ZB); braincase breadth (BB); postorbital constriction breadth (POB); palatal width at canines (C–C); mastoid width (MSTW); mastoid process width (MPW); palatal length (PL); maxillary toothrow length (MTRL); molariform toothrow length (MLTRL); width at the 3rd molar (M3–M3); dentary length (DENL); and mandibular toothrow length (MAND).

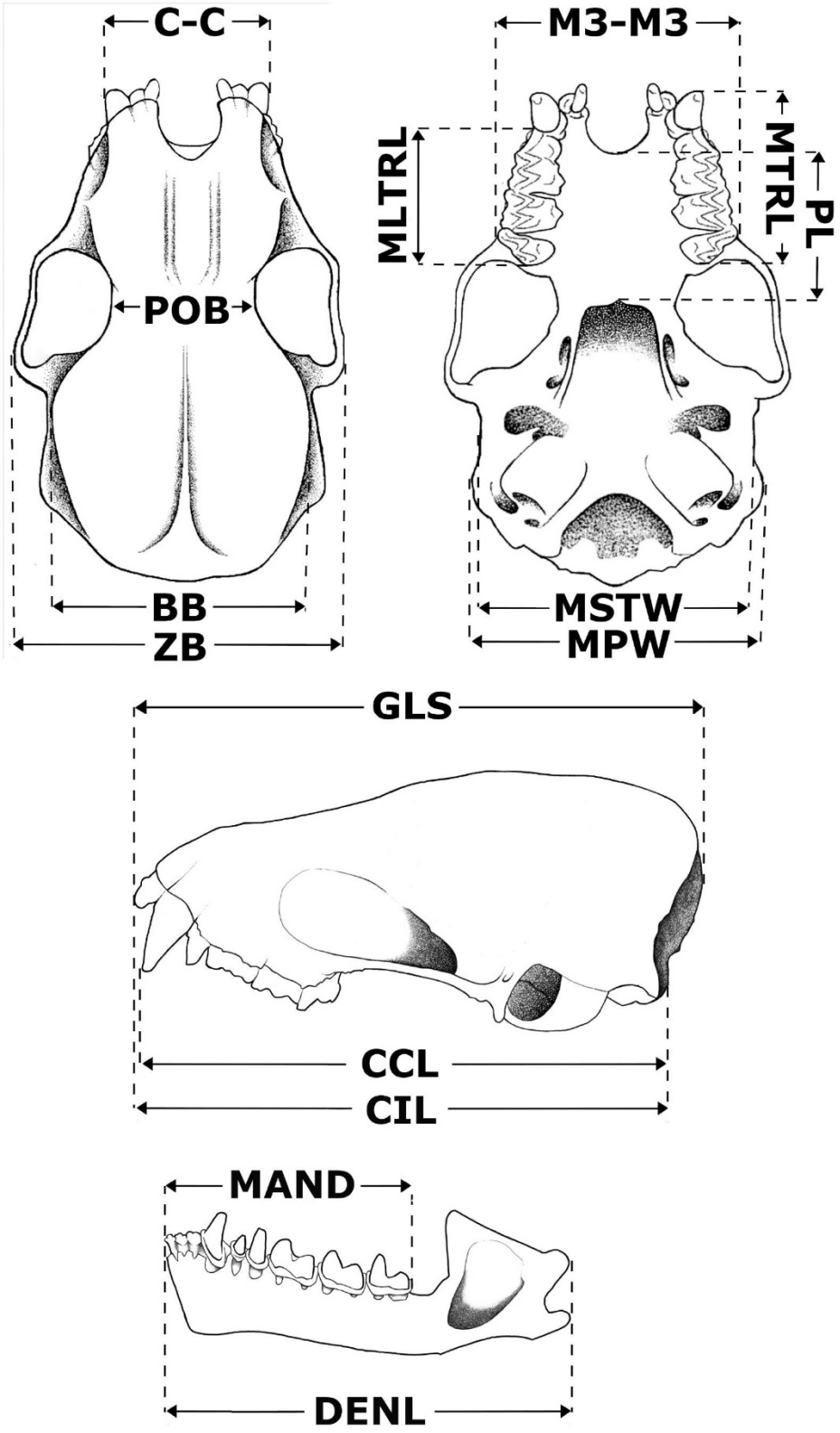

Figure 2. Cranial measurements illustrated on a skull of *Pseudoromicia*, labeled using their associated abbreviations. See Materials and Methods for complete list of measurement abbreviations.

We used the software SAS 9.4 (SAS Institute Inc., 2018) for all univariate morphological analyses. Species means, standard deviation, and range, were calculated using PROC Univariate; normality was assessed with the Normal option of the same procedure, using the Shapiro–Wilk test. Because a number of the measured variables were not normally distributed within sex and species, we used the PROC npar1way with the Wilcoxon option to assess sexual dimorphism – where numbers permitted this operation – in the species under consideration; as used, the procedure returns the results of a Wilcoxon signed-rank test (Wilcoxon, 1945). Dentary length (DENL) in *P. isabella* was found to be sexually dimorphic using the Wilcoxon test; width between upper canines (C–C) in *P. isabella* was deemed sexually dimorphic based on a *t*-test (SAS PROC ttest). Based on the otherwise overall lack of sexual dimorphism in the sample, sexes were combined to increase sample sizes for interspecific comparisons.

To assess potential differences in the measurements signifying specific distinction, we used a least squares approach to general linear models by using PROC GLM, invoking the MEANS/REGWQ option, which specifies the Ryan-Einot-Gabriel-Welsch multiple range test. This test controls for Type I error under each partial null hypothesis and is recommended for these types of biological comparisons (Day & Quinn, 1989; Ruedas, 1998). Groups identified with the same identifier (superscript letter) are not significantly different from each other, and groups identified by a different identifier are significantly different from other groups, with the proviso that some groups (i.e., species) may have membership in multiple groups, depending on the mean and variance of the measurement under consideration

Multivariate morphological analyses.— We undertook a Principal Components Analysis (PCA) to compare cranial morphology across *Pseudoromicia* species. Analyses were carried out in the

package ‘vegan’ (Oksanen et al., 2020), run in R version 4.2.0 (R Core Team, 2020) and plotted using ggplot2 (Wickham, 2016). Data were $\log_{10}$-transformed prior to the analysis; principal components were computed from the correlation matrix (Voss et al., 1990). We used only craniodental variables, and removed variables with data missing from numerous specimens, as well as one each from pairs of highly correlated variables. The final variable set employed included: GLS, CIL, MPW, POB, BB, MTRL, C–C, M3–M3, DENL, and MAND, and resulted in an ordination employing 66 of the 76 specimens. In addition, because *Pseudoromicia* species are morphologically cryptic and their limits uncertain, we repeated the PCA only with the newly collected individual and the 26 comparative specimens of *Pseudoromicia* whose taxonomic identity had been determined using molecular techniques (Monadjem, Richards, et al., 2021; Monadjem, Demos, et al., 2021). This resulted in both instances in analyses using 23 individuals with the same combination of mensural characters as above (three individuals were removed from the analysis due to missing variables).

DNA sequencing and phylogenetics.— Genomic DNA from the tissue sample of *Pseudoromicia* sp. (FMNH 240714) preserved in 95% ethanol was extracted using the DNeasy Blood and Tissue Kit (Qiagen). The mitochondrial Cytochrome *b* (*Cytb*) gene was selected for amplification using the primer pair LGL 765 F and LGL 766 R (Bickham et al., 1995, 2004). The PCR mixture included 12.5 µL of One*Taq*® Quick-Load® 2X Master Mix (New England Biolabs, Ipswich, MA, USA), 8.5 µL of water, 1 µL of each 10 µmol/L primer solution, and 2 µL of sample DNA. The PCR mixture was amplified as follows: initial 3 min at 94 °C; 38 cycles of 30 s at 94 °C, 45 s at 50 °C, and 90 s at 72 °C; then 7 min at 72 °C of final extension. Polymerase chain reaction product was purified using ExoSAP-IT (Thermo Scientific, Waltham, MA, USA). Sequencing

was undertaken in both directions on an ABI 3100 thermocycler (Applied Biosystems, Bedford, MA, USA) at the Pritzker Laboratory for Molecular Systematics and Evolution (FMNH). Chromatograms were edited and assembled in Geneious Prime 2022.0.2 (https://www.geneious.com; Biomatters Ltd, Auckland, New Zealand). Sequence alignments were made using Muscle (Edgar, 2004) with default settings in Geneious. Protein-coding sequence data from *Cytb* were translated to amino acids to confirm the absence of premature stop codons, insertions, and deletions. The newly generated sequence has been deposited in GenBank under accession number ON241266..

For *Cytb*, 31 *Pseudoromicia* sequences were extracted from the alignment generated by Monadjem, Demos, et al. (2021), then combined with the new sequence generated for this study (see Supplemental Appendix 2 for GenBank numbers). A sequence of *Afronycteris nana* (Peters, 1852; FMNH 192110; GenBank MT777850) extracted from the same alignment was used as an outgroup. Uncorrected *Cytb* sequence divergences (*p*-distances) among and within *Pseudoromicia* species were calculated using MEGA X v.10.1.7 (Kumar et al., 2018). jModelTest 2 v.2.1.10 (Darriba et al., 2012) on the CIPRES Science Gateway v.3.3 (Miller et al., 2010) was used to determine the sequence substitution models that best fit the data, and ranked according to the corrected Akaike information criterion (AICc). Maximum likelihood (ML) analysis was undertaken with the software IQ-TREE v.2.1.2 (Nguyen et al., 2015) in the CIPRES portal on an unpartitioned data set. Gene tree analyses using a Bayesian inference (BI) model were generated in MrBayes v.3.2.7 (Ronquist et al., 2012) in the CIPRES portal for the same alignment as the ML analysis. Two independent runs were undertaken in MrBayes using four Markov chains run for 5×10^6 generations under default heating values and sampled every 5000 generations. A conservative 25% burn-in was used, and stationarity of the results were assessed

using TRACER v1.7 (Rambaut et al., 2018). Majority-rule consensus trees were assembled for each Bayesian analysis.

RESULTS

Univariate analyses.— The 75 specimens of *Pseudoromicia* previously measured by Monadjem, Richards, et al. (2021) and the newly collected *Pseudoromicia* specimen from Mbam Minkom were used for uni- and multivariate analyses. The multiple range test identified significant differences among species, including those in the analysis that used only specimens that had previously been identified using molecular techniques (Monadjem, Richards, et al., 2021; Monadjem, Demos, et al., 2021). All species of *Pseudoromicia* examined are distinguishable based on combinations of the mensural variables employed here (Table 1; Figs 3 and 4). The most useful mensural character in discrimination of the new *Pseudoromicia* specimen from remaining congeners is mandibular toothrow (MAND; $F_7 = 18.22$, $P < 0.0001$; $R^2 = 0.662$), where the *Pseudoromicia* specimen from Cameroon displays one of the largest measurements, surpassed only by a single specimen of *P. roseveari*.

Table 1.—Univariate statistics, test of normality, and results of the Ryan–Einot–Gabriel–Welsch multiple range test for external and craniodental measurements of *Pseudoromicia* species. For each species, the top row (species label) also indicates the sample size (number in parentheses). Results displayed include mean ± standard deviation, sample size for each measurement (in parentheses) when different from the sample size of individuals examined for the species, and range (minimum value – maximum value). A "†" after the mean value indicates a non–normal distribution for that variable. Superscripts associated with the mean for the value identify statistically significantly different groups as judged by the Ryan–Eynot–Gabriel–Welsch multiple range test, arranged in order of descending size (a > b > c …). Stars by the character indicate the significance level of the character in the analysis of variance; **: <0.01; ****: <0.0001

Taxon → Character ↓	*P*. sp. n. (1)	*brunnea* (15)	*isabella* (6)	*kityoi* (2)
Mass****	6^{b}	$6.0^{\dagger a,b}$ ± 1.1 (14) 4.8 – 9.4	$4.7^{b,c}$ ± 0.9 4.0 – 6.0	8.0^{a} ± 0.1 7.9 – 8.0
Forearm****	$36^{a,b}$	34.6^{b} ± 1.1 (14) 32.8 – 36.7	30.6^{c} ± 1.5 28.0 – 31.9	37.5^{a} ± 0.7 37 – 38
Total length****	94^{a}	$84.6^{b,c}$ ± 3.2 (14) 80.0 – 89.0	$78.7^{c,d}$ ± 2.7 74.0 – 82.0	88.5^{b} ± 0.7 88 – 89
Tail length****	$39^{a,b}$	$35.8^{a,b}$ ± 1.6 (14) 33.0 – 38.0	29.3^{c} ± 4.2 24.0 – 36.0	$35.0^{a,b}$ ± 1.4 34 – 36

Ear length	12[a,b]	12.4[a] ± 0.8 (14) 11.0 – 14.0	12.3[a] ± 1.4 10.0 – 14.0	10.0[b] ± 0.0 10 – 10
Hind foot (c.u.)****	9[a,b]	8.1†[a,b,c] ± 1.5 (14) 7.0 – 12.0	6.9[b,c] ± 1.2 5.0 – 8.0	9.5[a] ± 0.7 9.0 – 10.0
GLS****	14.0[b]	13.7[b,c] ± 0.4 13.1 – 14.2	13.1[c,d,e] ± 0.1 (5) 13.0 – 13.3	14.8[a] ± 0.2 14.7 – 15.0
CI****	13.3[b,c]	12.9†[b,c,d] ± 0.4 (14) 12.2 – 13.4	12.5[c,d] ± 0.1 (5) 12.4 – 12.7	14.1[a] ± 0.2 13.9 – 14.2
C–C****	12.8[b]	12.7[b,c] ± 0.4 (10) 11.9 – 13.0	12.0[c,d] ± 0.2 (5) 11.8 – 12.2	13.6[a] ± 0.1 13.6 – 13.7
ZB****	9.4[a]	8.7[a,b,c] ± 0.5 (14) 7.7 – 9.6	8.3[b,c,d] ± 0.4 (5) 7.6 – 8.6	9.6[a] ± 0.1 9.5 – 9.6
MPW****	7.9[a,b]	7.5[b,c] ± 0.2 7.1 – 7.9	7.3[c,d] ± 0.2 (5) 7.0 – 7.5	8.2[a] ± 0.0 8.2 – 8.2
POB**	3.5[b]	3.9[a,b] ± 0.2 3.6 – 4.4	3.7[a,b] ± 0.2 (5) 3.5 – 3.9	4.0[a,b] ± 0.0 3.9 – 4.0
BB****	7.1[a,b]	7.1[a,b] ± 0.3 6.6 – 7.7	6.8[b,c] ± 0.2 (5) 6.5 – 6.9	7.6[a] ± 0.1 7.5 – 7.7

MTRL****	4.8[b,c,d]	4.9[b,c] ± 0.1 4.6 – 5.1	4.5[d,e] ± 0.0 (5) 4.4 – 4.6	5.2[a] ± 0.0 5.1 – 5.2
C–C****	4.3[a,b]	4.2[a,b] ± 0.2 3.6 – 4.6	4.4[a,b] ± 0.2 (5) 4.2 – 4.6	4.7[a] ± 0.1 4.6 – 4.7
M3–M3****	5.8[a,b]	5.9[a,b] ± 0.3 5.5 – 6.6	5.5[b,c] ± 0.1 (5) 5.3 – 5.6	6.1[a] ± 0.0 6.1 – 6.1
DENL****	10.2[b,c]	10.1[b,c] ± 0.3 (14) 9.4 – 10.7	9.6[c] ± 0.2 (5) 9.3 – 9.9	11.0[a] ± 0.3 10.8 – 11.2
MAND****	5.7[a]	5.3[a,b] ± 0.3 4.8 – 5.9	5.0[b,c] ± 0.2 (5) 4.9 – 5.4	5.6[a] ± 0.0[a] 5.6 – 5.6

Table 1.—extended

Taxon → Char ↓	*nyanza* (18)	*rendalli* (13)	*roseveari* (10)	*tenuipinnis* (11)
Mass****	6.1[a,b] ±1.0 (13) 4.8 – 8.3	5.8†[b,c] ± 0.9 (6) 4.0 – 6.8	6.5†[a,b] ± 0.5 6.0 – 7.0	4.0[c] ± 0.3 (6) 3.5 – 4.4
Forearm****	31.2[c] ± 1.2 (13) 29.0 – 33.0	34.8[a,b] ± 1.3 (9) 33.4 – 37.0	36.5†[a,b] ± 1.5 32.6 – 38.0	29.4[c] ± 1.2 (8) 28.1 – 32.0
Total length****	83.5[b,c] ± 2.7 (13) 79.0 – 89.0	88.6[a,b] ± 3.9 (8) 82.0 – 95.0	87.3[b] ± 2.9 83.0 – 93.0	74.2[d] ± 2.2 (5) 72.0 – 77.0
Tail length****	33.3[b,c] ± 2.3 (13) 30.0 – 38.0	37.0[a,b] ± 3.2 (9) 32.0 – 42.0	39.7[a] ± 2.6 34.0 – 44.0	29.2[c] ± 0.8 (5) 28.0 – 30.0
Ear length	12.1†[a,b] ± 0.6 (13) 11.0 – 13.0	11.3[a,b] ± 1.6 (9) 9.0 – 13.0	12.9†[a] ± 0.6 (8) 12.0 – 14.0	12.7[a] ± 0.8 (7) 12.0 – 14.0
Hind foot (c.u.)****	7.5†[a,b,c] ± 0.7 (13) 7.0 – 9.0	7.5[a,b,c] ± 0.9 (8) 6.0 – 9.0	9.9†[a] ± 1.1 8.0 – 11.0	6.4†[c] ± 0.8 (7) 5.0 – 7.0
GLS****	13.0[d,e] ± 0.2 (17) 12.5 – 13.4	13.6[b,c,d] ± 0.5 (12) 13.0 – 14.7	14.1†[b] ± 0.4 13.4 – 14.5	12.4[e] ± 0.3 (10) 12.0 – 12.8

CI****	12.2[d,e] ± 0.3 (17) 11.4 – 12.6	13.0[b,c,d] ± 0.4 (12) 12.4 – 13.8	13.4[b] ± 0.5 12.6 – 14.0	11.7[e] ± 0.3 (10) 11.1 – 12.1
C–C****	11.8[d] ± 0.3 (17) 11.1 – 12.2	12.7[b,c] ± 0.3 (7) 12.3 – 13.2	13.3[a,b] ± 0.0 (2) 13.3 – 13.3	11.3[d] ± 0.4 (6) 10.6 – 11.6
ZB****	8.0[c,d] ± 0.3 (17) 7.5 – 8.7	9.0[a,b] ± 0.4 (10) 8.4 – 9.9	8.8[a,b,c] ± 0.5 (9) 8.0 – 9.5	7.5[d] ± 0.5 (9) 6.8 – 8.2
MPW****	7.3[c,d] ± 0.2 (17) 7.0 – 7.8	7.8[a,b,c] ± 0.3 (12) 7.2 – 8.3	7.8[a,b] ± 0.2 7.5 – 8.4	6.9†[d] ± 0.1 (10) 6.8 – 7.2
POB**	4.0†[a] ± 0.2 (17) 3.7 – 4.7	4.0[a] ± 0.1 (12) 3.8 – 4.2	3.8[a,b] ± 0.2 3.5 – 4.1	3.8†[a,b] ± 0.2 (10) 3.5 – 4.2
BB****	7.0†[b,c] ± 0.2 (17) 6.7 – 7.4	7.2[a,b] ± 0.3 (12) 6.8 – 7.8	7.3[a,b] ± 0.3 6.9 – 7.8	6.5†[c] ± 0.1 (10) 6.4 – 6.8
MTRL****	4.3[e] ± 0.1 (17) 4.0 – 4.5	4.7[c,d] ± 0.2 (12) 4.4 – 5.1	5.0[a,b] ± 0.2 4.8 – 5.3	4.2†[e] ± 0.1 3.9 – 4.4
MLTRL****	4.1[b,c] ± 0.1 3.9 – 4.3	4.4[a,b] ± 0.2 (12) 4.0 – 4.8	4.3[a,b] ± 0.2 3.8 – 4.7	3.8[c] ± 0.3 (10) 3.3 – 4.1
M3–M3****	5.2[c,d] ± 0.2 4.9 – 5.5	5.8[a,b] ± 0.3 (10) 5.1 – 6.2	6.0[a,b] ± 0.2 5.5 – 6.3	5.0[d] ± 0.2 (10) 4.7 – 5.3

DENL****	9.1[d] ± 0.2 8.8 – 9.5	10.0[b,c] ± 0.3 (12) 9.4 – 10.5	10.4†[b] ± 0.3 (9) 9.8 – 10.7	8.8[d] ± 0.4 8.2 – 9.3
MAND****	4.6[c] ± 0.1 4.4 – 4.8	5.1[b,c] ± 0.2 (12) 4.6 – 5.5	5.2†[a,b] ± 0.3 (9) 5.0 – 6.0	4.6†[c] ± 0.2 4.4 – 5.2

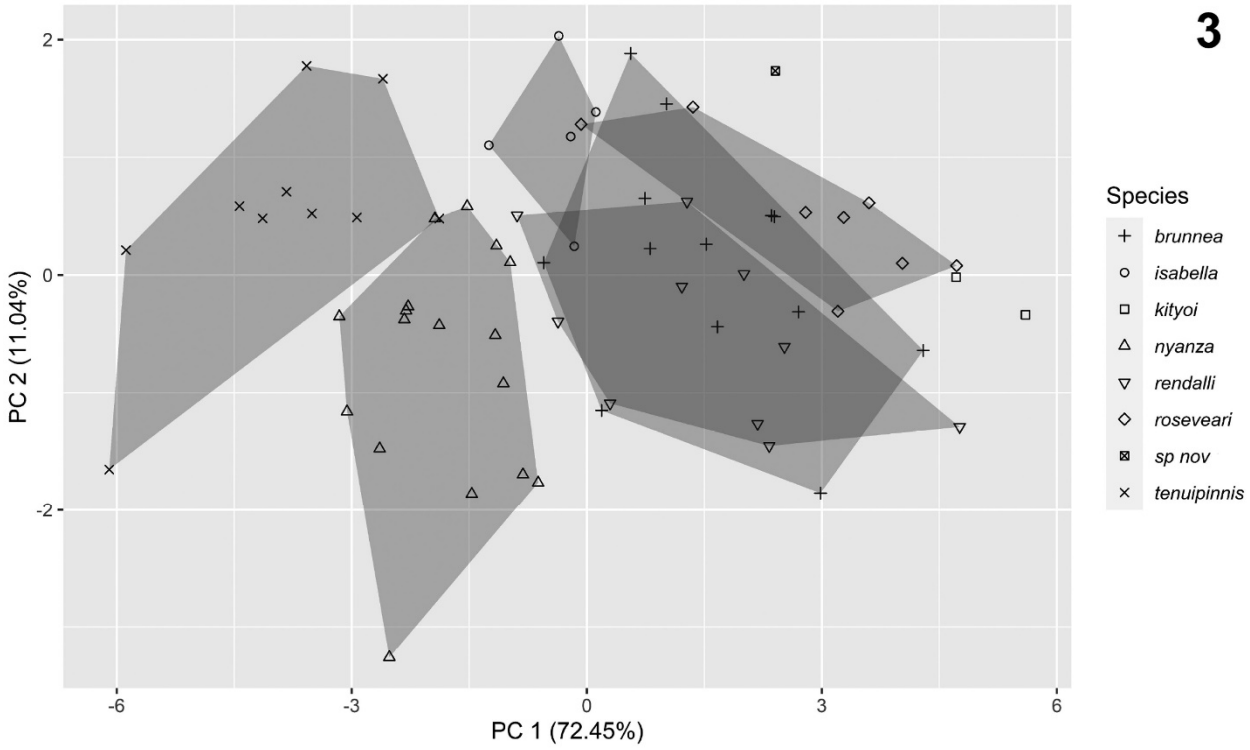

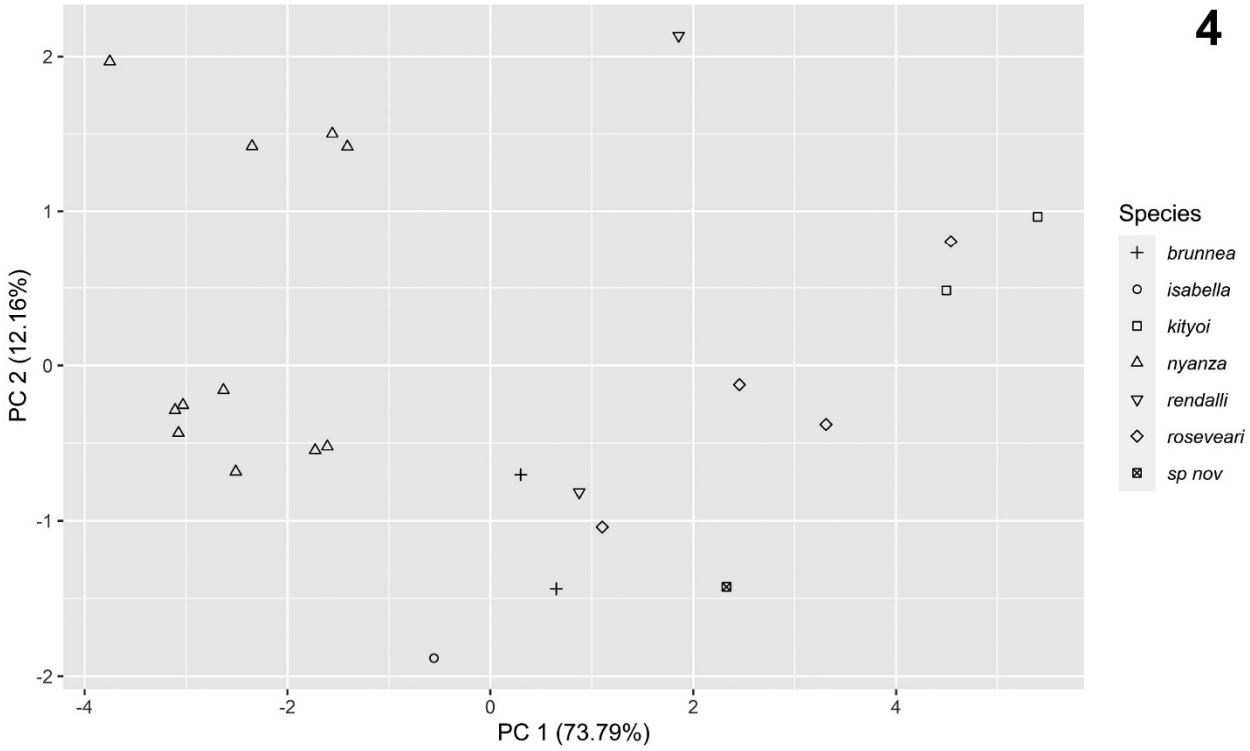

Figures 3 and 4. (3 [top]) Graphical results of the Principal Components Analysis based on log10–transformed variables, computed from the correlation matrix, for all specimens examined with all the mensural characters available (66 of 77 specimens with all the following characters: GLS, CIL, MPW, POB, BB, MTRL, C–C, M3–M3,

DENL, and MAND) (3). Only the first two Principal Components are significant: PC1 accounts for 72.45% of the variation; PC2, 11.04%. (4 [bottom]) Graphical results of the Principal Components Analysis based on log10–transformed variables, computed from the correlation matrix, for specimens examined for which taxonomic identity had been established previously using sequence data (Monadjem et al. 2021a, b; this work) with all the mensural characters available (23 of 26 specimens with the following: GLS, CIL, MPW, POB, BB, MTRL, C–C, M3–M3, DENL, and MAND). Only the first three Principal Components are deemed significant; PC1 accounts for 73.79% of the variation; PC2, 12.16%; PC3, 4.60%

Table 2.— Eigenvector loadings of the principal components analysis (PCA) for principal component (PC) 1 and PC 2, based on natural log-transformed craniodental measurements of the currently recognized species of *Pseudoromicia*, following the taxonomic arrangement of Monadjem et al. (2021). "Proportion" and "cumulative" refer to the proportion of the variance explained by each of the principal components, and the cumulative variance explained by the first two (all specimens) or three (sequenced specimens) principal components, respectively.

	All specimens		Sequenced specimens		
	PC1	PC2	PC1	PC2	PC3
GLS	0.3582	-0.0069	0.3533	0.0069	0.1107
CI	0.3565	-0.0346	0.3454	0.0002	0.1868
MPW	0.3278	0.2083	0.3202	0.2515	-0.4800
POB	0.0314	0.8967	-0.1280	0.7797	0.5136
BB	0.2943	0.3036	0.2798	0.4618	-0.5198
MTRL	0.3387	-0.1579	0.3559	-0.0428	0.0908
C–C	0.3077	-0.0432	0.3095	0.1733	0.2612
M3-M3	0.3383	-0.0874	0.3077	-0.2376	0.1785
DENL	0.3594	-0.1198	0.3573	-0.0841	-0.0066
MAND	0.3107	-0.1017	0.3373	-0.1414	0.2830
Eigenvalue	7.2452	1.1041	7.3955	1.2001	0.4611
Proportion	0.7245	0.1104	0.7395	0.1200	0.0461
Cumulative	0.7245	0.8349	0.7395	0.8596	0.9057

Principal components analysis.— Based on the scree plot from the PCA, only the first two principal components were significant in the PCA that included all specimens (Fig. 3). Principal component (PC) 1 accounted for 72.45% of the variation; PC2 for 11.04% (cumulative percent: 83.49%). In the PCA that included only molecularly identified specimens (Fig. 4), PC1 accounted for 73.79% of the variation and PC2 for 12.16% (cumulative percent: 85.95%). With the exception of postorbital breadth, eigenvectors in PC1 were relatively homogeneous (); we thus interpret this axis as generally representative of size. This can be confirmed by visual inspection of the results (Figs 3 and 4), which locate *P. tenuipinnis* and *P. nyanza*, generally the smallest in most craniodental variables examined, toward the smallest values of PC1, and *P. kityoi* and *P. roseveari*, with generally larger measurements, at the opposite end of the ordination. Confirming the results of the multiple range test, the specimen from Cameroon is highly distinct from remaining *Pseudoromicia* species in PC2. The largest coefficients of PC2 are those of postorbital breadth and breadth of braincase, therefore suggesting that the *Pseudoromicia* specimen from Cameroon has an exceptionally narrow postorbital constriction and a relatively narrower braincase than other *Pseudoromicia* species (Figs 3 and 4; Table 1).

Table 3.—Uncorrected cytochrome *b* *p*-distances among (below diagonal) and within (numbers on diagonal, in bold) 9 species of *Pseudoromicia* calculated in MEGA X v.10.0.5.

	brunnea	*isabella*	*kityoi*	*mbamminkom*	*nyanza*	*rendalli*	*roseveari*	sp. Tanzania
brunnea	**0.002**							
isabella	0.096	**na**						
kityoi	0.086	0.095	**0.004**					
mbamminkom	0.083	0.086	0.052	**na**				
nyanza	0.129	0.139	0.146	0.134	**0.008**			
rendalli	0.129	0.148	0.142	0.139	0.140	**0.018**		
roseveari	0.079	0.093	0.051	0.051	0.131	0.137	**0.005**	
sp. Tanzania	0.088	0.092	0.083	0.066	0.147	0.147	0.076	**na**

Genetic evidence.— The MrBayes MCMC analysis converged successfully, with all parameter effective sample sizes (ESS) >1000. The mitochondrial alignment contains 1134 characters (16% missing characters, sequence lengths = 490 – 1120 ungapped bases) and 33 individuals. Following the jMODELTEST results, we applied the GTR + Γ model for ML and BI analyses. Our resulting gene tree (Fig. 5) places the Cameroon *Pseudoromicia* as a member of a weakly supported clade that includes *P. roseveari* and *P. kityoi* (posterior probability (PP) = 0.82, bootstrap (BS) = 68%). The shallowest well-supported node (PP = 1.0, BS = 99%) that includes the new *Pseudoromicia* is a clade that comprises *P. roseveari*, *P. kityoi*, *Pseudoromicia* sp. nov., the undescribed species from Tanzania, *P. brunnea*, and *P. isabella*. As a result, the closest sister taxon to *P.* sp. nov. is unresolved. All *Pseudoromicia* species represented by two or more sequences are well supported as monophyletic (PP = 1.0, BS = 100%). The new species differs from other *Pseudoromicia* species with *p*-distances of 5.1 − 13.9% (Table 3).

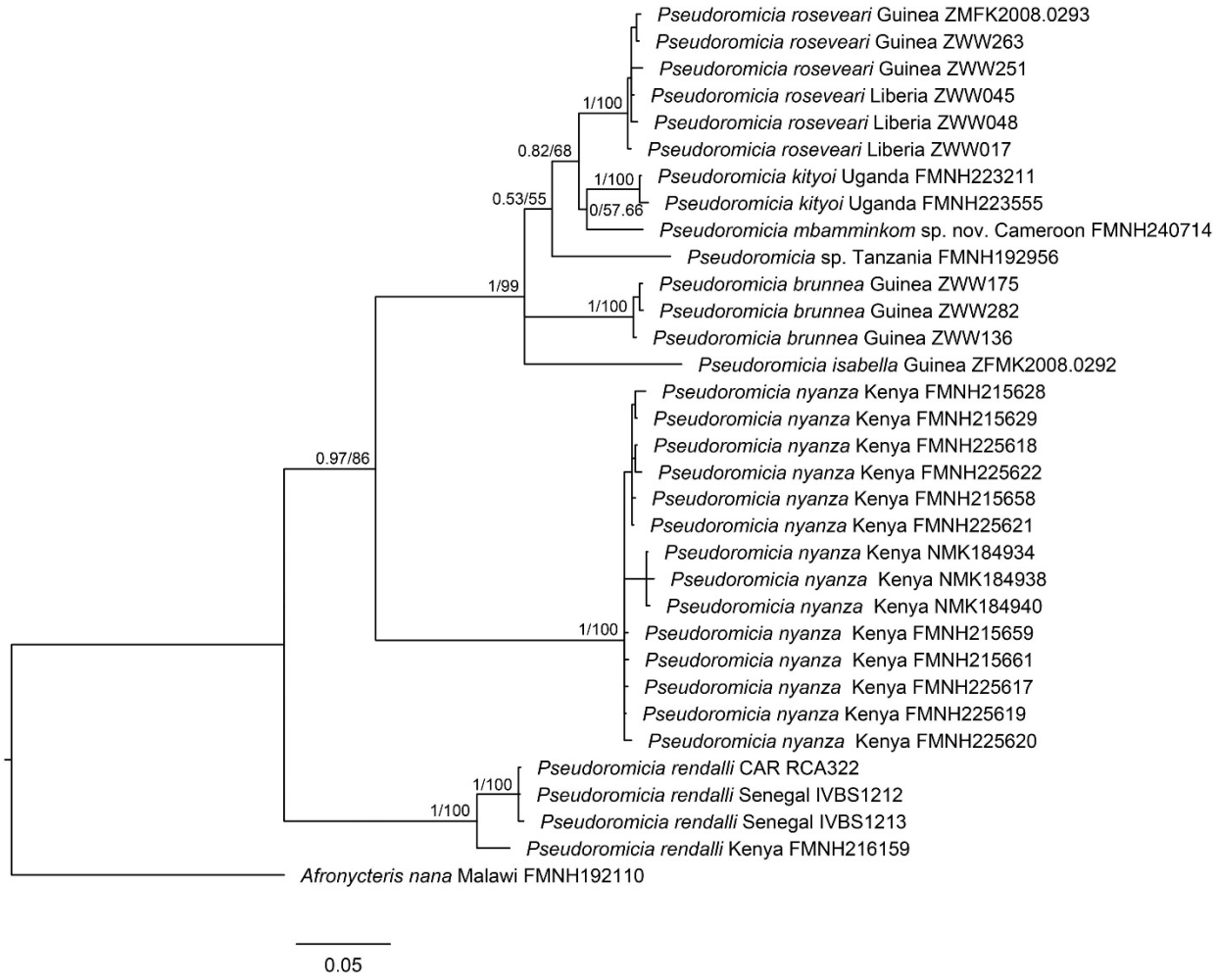

Figure 5. Bayesian phylogeny based on mitochondrial Cytochrome *b* sequences of *Pseudoromicia*. The phylogeny was inferred in MrBayes and its topology was very similar to the maximum-likelihood phylogeny inferred in IQ-TREE. Values at nodes denote Bayesian posterior probabilities (PP) followed by bootstrap support (BS). Tips of the phylogeny are labeled with specimen information: species, country, and voucher number, or GenBank number where voucher number is unavailable. All GenBank numbers are provided in Supplemental Appendix 1.

On the basis of the foregoing results, we hypothesize that the Cameroon specimen of *Pseudoromicia* constitutes an undescribed species, that we describe below as:

FAMILY VESPERTILIONIDAE GRAY, 1821

SUBFAMILY VESPERTILIONINAE GRAY, 1821

TRIBE VESPERTILIONINI GRAY, 1821

GENUS *PSEUDOROMICIA* MONADJEM, PATTERSON, WEBALA, AND DEMOS, 2021

***Pseudoromicia mbamminkom* sp. nova**

Mbam Minkom Serotine

Figs 7–13, Table 4

Holotype: FMNH 240714, adult female, not pregnant or lactating. Body preserved in ethanol, with skull extracted and cleaned. Specimen collected by ALG, YN, and LAR, on 14 August 2019; field catalogue number ALG 23.

Type locality: Cameroon: Centre Region, Lekié Department; NW slope of Mount Mbam Minkom, 3°58.156'N, 11°22.840'E (datum: WGS84), 785 m, near the village of Nkolakie (also spelled Nkolakié); the locality is illustrated as Camp 2 in Fig. 1. The specimen was collected in secondary forest, using a mist net set across the Bitemgu River.

Etymology: A noun in apposition, named for the type locality, the most prominent summit in its namesake Mbam Minkom Massif, an isolated gneiss inselberg formation emerging from the surrounding lowland forest matrix.

Distribution: Based on a single record at an elevation of 785 m on Mount Mbam Minkom in the Centre Region of Cameroon (Fig. 1).

Diagnosis: *Pseudoromicia mbamminkom* is a large-sized member of the genus *Pseudoromicia* (Table 1, Figs. 3, 4, 6). A dark brown muzzle and wings distinguish it from the white-winged members of the genus (*P. isabella*, *P. rendalli*, *P. nyanza*, and *P. tenuipinnis*). It is similar in size and appearance to its putative sister species *P. kityoi*; however, cranially, *P. mbamminkom* and *P. kityoi* differ in the lateral view: the dorsal aspect of the rostrum is angled continuously from the braincase in *P. mbamminkom* while being markedly depressed in *P. kityoi* (Fig. 7). The rostral facies of the palatal emargination, or notch, is rounded and scallop-shaped in *P. mbamminkom*, but narrower and U-shaped in *P. kityoi*. The occipital condyles are more ventrally pronounced in *P. mbamminkom* and the inion is unobtrusively rounded in contrast with the markedly prominent inion in *P. kityoi*. The caudal midline projection of the palatine bone is lacking in *P. mbamminkom* but present in the holotype of *P. kityoi*; however, this may be an intraspecifically variable character in other taxa and should be evaluated further with additional specimens. Dentally, the cingulum surrounding the lingual aspect of I1 is continuous in *P. mbamminkom*, and broad in proportion to width of the incisor (Figs. 8 and 9). The cingulum is narrower and discontinuous between the lingual and labial aspects in *P. kityoi*. The hypocone basin in PM2 is reduced in *P. mbamminkom* with respect to *P. kityoi*. Lower m1 and m2 in *P. kityoi* have a broadly extended posterior lingual shelf not present in *P. mbamminkom*. Although overlapping in individual cranial variables with other members of *Pseudoromicia* (Table 1), it can be distinguished more easily by means of the PCA of cranial dimensions (Figs. 3 and 4), in particular along PC2, which loads most heavily on breadth of postorbital constriction and braincase, as well as mastoid breadth. Indeed, *P. mbamminkom* has the narrowest interorbital region of known *Pseudoromicia* species. In addition, *P. mbamminkom* is distinguished

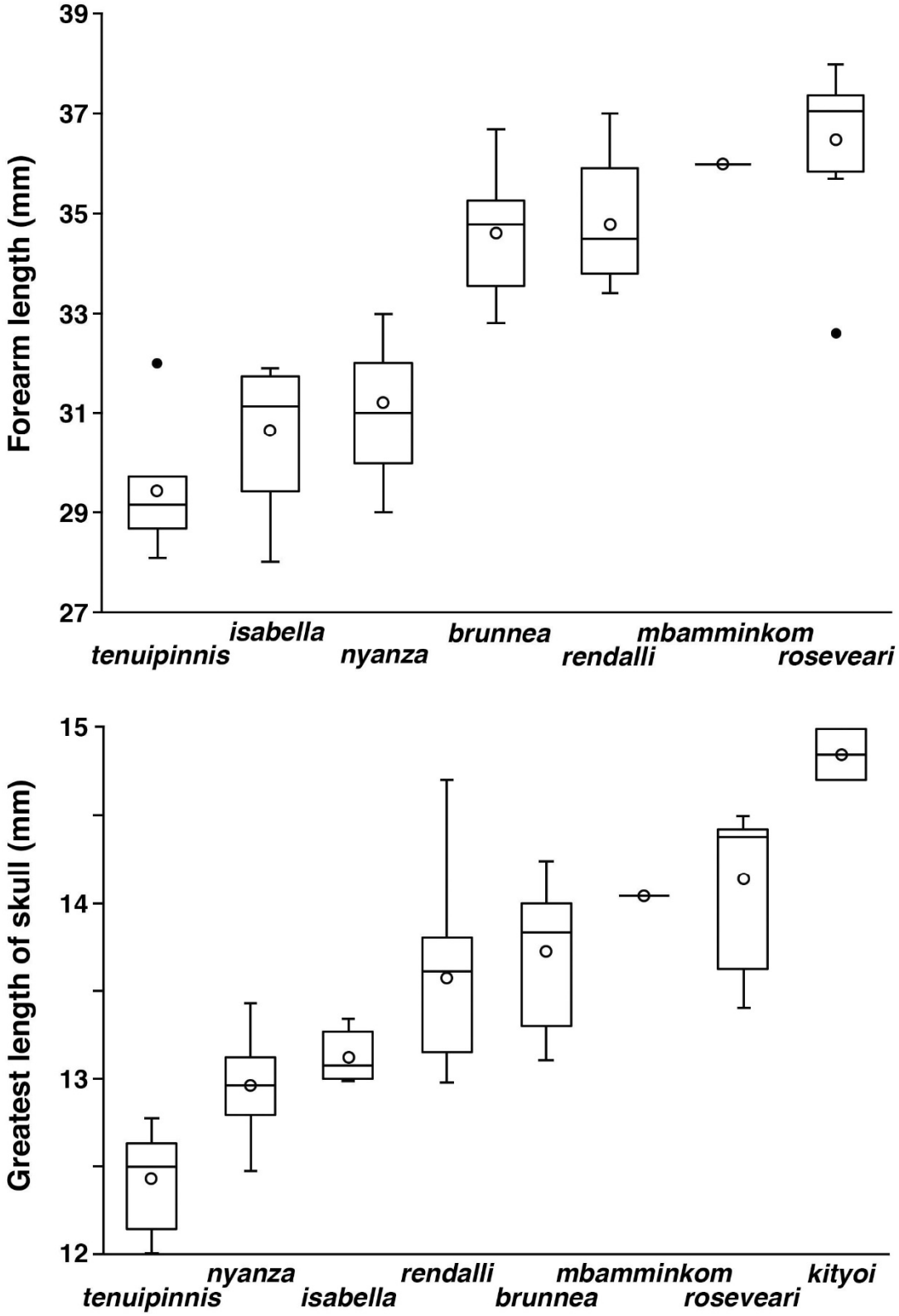

Figure 6. Box and whisker plot comparing the size and magnitude of variation within and across species of *Pseudoromicia* in forearm length (top) and greatest length of skull (bottom).

Figure 7. Dorsal, ventral, and lateral view of the skull of the holotype of *Pseudoromica kityoi* (right) and the holotype of *Pseudoromicia mbamminkom* sp. nov. (left).

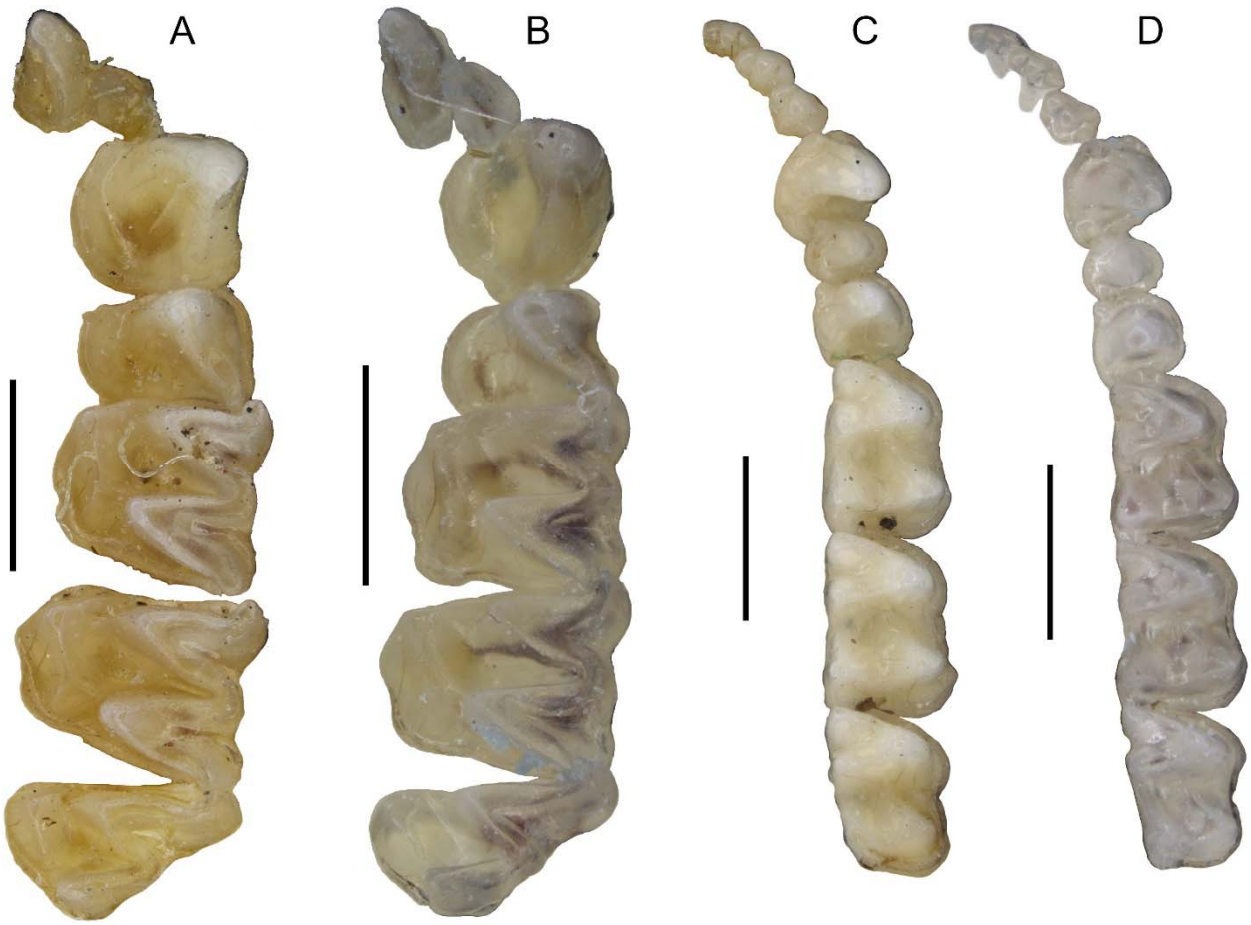

Figure 8. Scanning electron micrograph (composite) of the upper (left) and lower (right) dentition of *Pseudoromicia mbamminkom* sp. nov. (not to scale). Length of upper toothrow: 4.75 mm; length of lower toothrow: 5.68 mm.

Figure 9. Comparison of the upper and lower dentition of *Pseudoromicia mbamminkom* sp. nov. (holotype, FMNH 240714) to its hypothesized sister species, *P. kityoi* (paratype, FMNH 223211); A: upper dentition of *P. mbamminkom* sp. nov., B: upper dentition of *P. kityoi*, C: lower dentition of *P. mbamminkom* sp. nov., and D: lower dentition of *P. kityoi*. Scale bar = 1 mm.

genetically from other members of *Pseudoromicia* by a number of mitochondrial *Cytb* substitutions (Table 3).

Description: The only known specimen of *Pseudoromicia mbamminkom* is a large-sized pipistrelle-like bat (external and craniodental measurements listed in Table 1; wing measurements in Table 4). The dorsal pelage is reddish-brown (Sepia; Color 219 of Smithe, 1974) with uniformly coloured hairs ~5.0 mm in length (Fig. 10). The ventral pelage is bicoloured and slightly shorter (~4.0 mm) than the dorsal pelage. Individual ventral hairs are reddish-brown (Sepia; Smithe, 1974) at the base with tips of drab grey (Drab-grey; Colour 119 D of Smithe, 1974) eventually fading into uniformly coloured drab-grey nearing the uropatagium (Fig. 11). The wing and tail membranes are dark brown, as are the muzzle and ears. Ear length is typical for *Pseudoromicia*: 12 mm (vs. 12.2 ± 1.11, 9–14 mm across other species in the genus) and rounded. The tragus is broad (2.9 mm), blunt, and 7.0 mm in length, with a curved outer margin typical of the genus (Monadjem et al., 2013; Monadjem, Richards, et al., 2021 [as *Neoromicia*]; Fig. 12). The plagiopatagium attaches at the metatarsals, and a keeled calcar is present (Fig. 13). In lateral profile, the cranium is relatively flat (Fig. 7), and the rostrum angled continuously from the braincase. Sagittal and lambdoidal crests are absent. *Pseudoromicia mbamminkom* has a dental formula typical of the genus, I 2/3, C 1/1, P 1/2, M 3/3 = 32. I^1 is unicuspid and I^2 slightly less than half the length of I^1. P^1 is absent; the single upper premolar present in the toothrow is homologous with P^2.

Figure 10. Dorsal view of the body of the holotype of *Pseudoromicia mbamminkom* sp.nov. The frosted look is an effect of the lighting: the coloration is homogeneous.

Figure 11. Ventral view of the body of the holotype of *Pseudoromicia mbamminkom* sp. nov.

Figure 12. Pinna and tragus of the holotype of *Pseudoromicia mbamminkom* sp. nov.

Figure 13. Holotype of *Pseudoromicia mbamminkom* sp. nov.: detail of the uropatagium with keeled calcar and plagiopatagium attached at the metatarsals.

Biology: Because *Pseudoromicia mbamminkom* is known only from a single specimen, almost nothing can be said about the biology of the species. There is weak support suggesting *P. mbamminkom* as sister to *P. kityoi*. Like this new species, *P. kityoi* is only known from a single locality in the Mabira Forest Reserve in the Central Region of Uganda (0°26.706′N, 32°53.3256′E; ~1120 m asl) where two specimens were collected. The holotype of *P. mbamminkom* was not in an obviously reproductive status at the time of collection. No information other than that presented above is available on the biology of *P. mbamminkom*.

DISCUSSION

Biogeography.— The type locality for *P. mbamminkom* (Fig. 14) is approximately equidistant between Mabira Forest Reserve in Uganda (0°26.706′N, 32°53.3256′E), type locality of *P. kityoi*; ~2426 km), and Mt. Nimba (07°29′N, 08°35′W), on the Liberia–Guinea–Sierra Leone border; type locality of *P. roseveari* ~2257 km). Notwithstanding the lack of resolution in our molecular analyses, these data, albeit based on a single mitochondrial locus, suggest *P. kityoi* as sister to *P. mbamminkom*, but also places it definitively in a clade with *P. roseveari* and *P. kityoi*. This association suggests that the three species may be relicts of a single widespread species that originated in West Africa ("white-winged" group) then spread east across the tropical moist broadleaf forest reaching into East Africa, and now are restricted to a few upland rainforest patches in West Africa (*P. roseveari*), in outliers of the Cameroon Volcanic Line region (*P. mbamminkom*), and the Lake Victoria area (*P. kitoyi*). The smaller, white-winged species are hypothesized to be ancestral based on our molecular results, and the larger, dark-winged taxa dispersed to East Africa then back to West Africa (e.g., *P. mbamminkom*, *P. roseveari*). This also illustrates the potential biogeographic importance in this group of species of the Dahomey gap, the zone of aridity in Togo, Benin, and neighbouring states, between the Volta and Wemé Rivers, that breaks up the rainforest into Upper and Lower Guinea Rainforests.

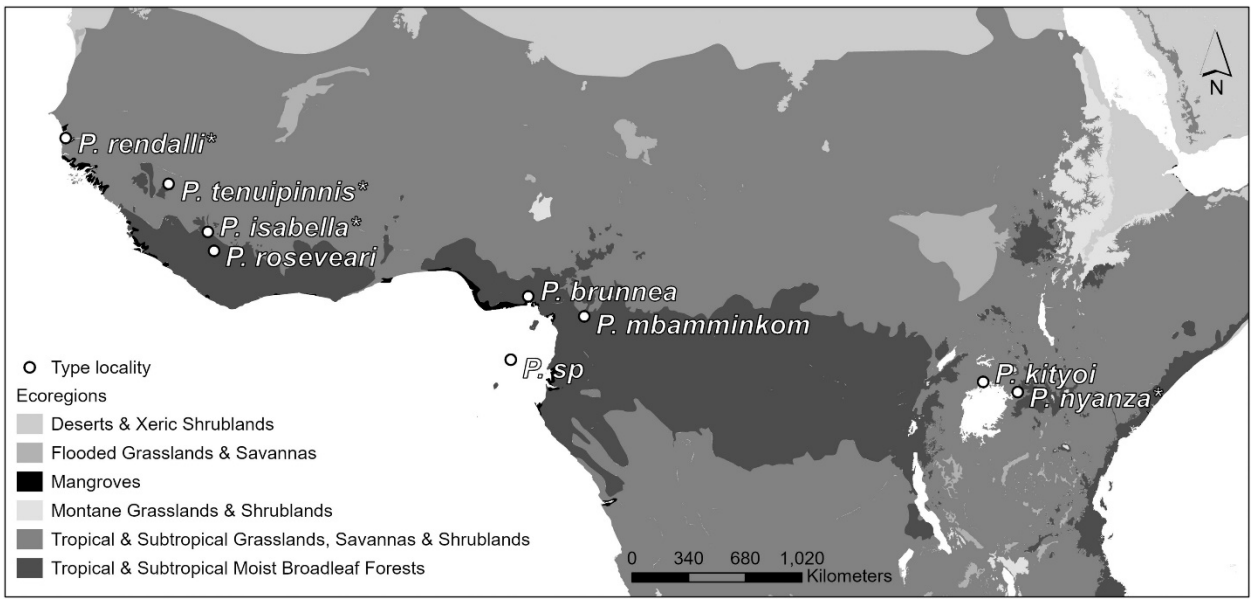

Figure 14. Map of the type localities of *Pseudoromicia* species. Species marked with an asterisk (*) are part of the white-winged group. Map created using ArcGIS software by Esri (2020); basemap created by subsetting ESRI's RESOLVE Ecoregions dataset (2017) containing 846 terrestrial ecoregions grouped into 14 biomes.

The Dahomey Gap has long been acknowledged as a significant biogeographic barrier (e.g., Booth, 1954, 1958; Grubb, 1978; Moreau, 1969). The genetic distances between each of these three species (Table 3; 5.2% to *P. kityoi* and 5.1% to *P. roseveari*; 5.1% between *P. kityoi* and *P. roseveari*), based on their magnitude, are more supportive of the hypothesis of Robbins (1978), who proposed a biogeographic barrier role for the Volta and Niger Rivers, rather than the arid vegetation belt as the primary vicariant mechanism (Booth, 1958). The presence of the arid belt is hypothesized to be relatively recent (9 − 4.5 KYA; Demenou et al., 2018). However, successive cycles of xeric and mesic climates leading to deforestation and reforestation (Carcasson, 1964; Demenou et al., 2016, 2018; Livingstone, 1975; Lönnberg, 1929; Moreau, 1952, 1963, 1966; Rowan et al., 2016) indicate that the arid corridor also may have played a vicariant role during glacial cycles. Notwithstanding, the presence of the Dahomey Gap, and the

Volta, Wemé, and Niger Rivers, all would reinforce the distinction between the faunas of Central and West African mountains, leaving what Grubb (1978: 159) called a “remarkable affinity between East African and Cameroon highland fauna”.

. However, successive cycles of xeric and mesic climates leading to deforestation and reforestation (Lonnberg 1929; Moreau 1962, 1963, 1966; Carcasson 1964; Livingstone 1975; Rowan et al. 2016; Demenou et al. 2016, 2018) indicate that the arid corridor also may have played a vicariant role during glacial cycles. Notwithstanding, the presence of the Dahomey Gap, and the Volta, Wemé, and Niger Rivers, all would reinforce the distinction between the faunas of Central and West African mountains, leaving what Grubb (1978:159) called a “remarkable affinity between East African and Cameroon highland fauna”.

In recent years, a large number of African bat species either have been described or documented without being formally described (e.g., 12 undescribed species of *Rhinolophus*, including sympatric morphologically cryptic species: Demos et al., 2019; 11 undescribed clades of *Miniopterus*: Demos et al., 2020). This suggests that the Afrotropical bat fauna, although characterized as depauperate relative to other tropical regions, likely has been under-studied and under-sampled (Herkt et al., 2016; Tanshi et al., 2022a), particularly in morphologically conservative groups such as vespertilionid bats. This work supports the aforementioned studies in proposing that there is higher bat species richness in Africa than has been intimated in taxonomic compendia and emphasizes the need for additional taxonomic sampling and comprehensive phylogenetic studies. This phenomenon is further exemplified when considering recent systematic work focused on African pipistrelle-like bats, which has revealed high levels of cryptic diversity in the group (Hutterer et al., 2019; Monadjem, Demos, et al., 2021). The tropical African bat fauna currently is considered to contain fewer species than that of tropical

regions of South America or Southeast Asia (Tanshi et al., 2022b). However, the accelerating rate of bat species discovery in Africa led Patterson et al. (2021) to suggest that, far from the 224 species known to Happold and Happold (2013; Van Cakenberghe and Seamark, 2021, list 344 extant species), the actual number of bats on the African continent "will eventually exceed 400 species of bats".

Conservation.— Conservation of Mbam Minkom's forests is vital to the preservation of biodiversity in Cameroon as well as to the economic and ecological stability of neighbouring communities. The Mbam Minkom Massif (MMM), covering ~4500 ha, is bisected by several springs, streams, and river gorges, all taking their rise from the mountain, thereby making it a major water catchment for the surrounding area and beyond. It not only provides clean water, but also is a major source of livelihood for at least 10 adjacent fringing villages. MMM is a region of exceptional ecological and economic importance, yet the fauna remains poorly studied. Because of human–wildlife conflicts, subsistence hunting, and over-harvesting resulting in habitat loss, large mammals are extremely rare. However, the remaining forest fragments still harbour charismatic flagship species of global conservation concern, such as one of the few remaining populations of Grey-necked Rockfowl (*Picathartes oreas*; Passeriformes: Picathartidae) and Giant Ground Pangolin (*Smutsia gigantea*; Pholidota: Manidae). Notwithstanding its enormous natural value, the MMM ecosystem is one of the most endangered in Cameroon because of the lack of legal conservation frameworks and exposure to increasing human pressure from the nearby (8 km) capital city, Yaoundé (Simo et al., 2009).

Based on the very limited information available to us on *P. mbamminkom*, the new species should be considered by IUCN as Data Deficient. Notwithstanding, the extent of

occurrence may be less than 100 km^2, based on the extent of forest and upland habitat constituting the MMM. In addition, at present, the species is known to exist only at a singular location; thus, there is an urgent need to determine whether this apparent geographic restriction and uncommonness is real or artefactual. The area, extent, and/or quality of habitat was observed to be declining. As a result of our assessment of conditions on the ground, *P. mbamminkom* may be facing a higher risk of extinction in the wild than its IUCN designation of DD would suggest. Certain taxa that were either unassessed by the IUCN, or Data Deficient, were found recently to be considerably more likely to be threatened than assessed species (Caetano et al., 2022). Similarly, over half of all DD species sampled – including over 60% of mammals – have been predicted to be threatened by extinction (Borgelt et al., 2022). The rapidly shrinking forest habitat of the Mbam Minkom Massif likely is cause for concern with respect to the conservation status of all the flora and fauna of the region: at least one other mammal species – *Leimacomys buettneri*, the Togo mouse, (Rodentia: Muridae) – representing a monotypic subfamily (Leimacomyinae) and known by two specimens from a single locality in Togo, has been hypothesized to be extinct in similar habitat under similar conditions of habitat degradation (Amori et al., 2016), and has not been rediscovered despite at least two expeditions dedicated to searching for it.

The recent systematic evaluations of vespertilionids, and in particular pipistrelle-like vespers, have resulted in the illumination of vast amounts of previously unresolved taxonomic diversity. We hope that our description of an additional member of *Pseudoromicia* will encourage further efforts to more closely examine currently existing specimens and continue surveying under-sampled regions in Africa to assess species boundaries, and to resolve the

taxonomy of other cryptic lineages in vespertilionids. These efforts are essential to the conservation of bat diversity in Cameroon in particular, as well as Africa as a whole.

ACKNOWLEDGEMENTS

We thank the Cameroon Ministry of Scientific Research and Innovation for kindly granting us research and collecting permits to undertake the research described herein (permits 96–99 of year 2019), and the Ministry of Forestry and Wildlife for permission to export our specimens (permit no. 1538 of year 2019). We thank Jan Decher for his guidance and moral support, as well as providing material support from the Alexander Koenig Zoological Research Museum (Bonn, Germany). We are immensely thankful to the communities surrounding Mount Mbam Minkom, who provided access, assistance, and accommodation; and in particular our host family in Nkolakié. We thank The Field Museum's Pritzker Laboratory staff for providing exceptional training in molecular techniques and use of their laboratory space and equipment. We thank the Collaborative Invertebrate Laboratories at the Field Museum and Dr C. Moreau for use of the imaging equipment (National Science Foundation, Negaunee foundation), and S. Ware, Manager Morphology Laboratories, for taking the dental light photographs. We also thank J. H. French of the U.S. Fish and Wildlife Forensic Laboratory (Ashland, Oregon) for taking the scanning electron micrograph of the dentition of the holotype of *P. mbamminkom*.

FUNDING

Funding of this research for ALG came from Portland State University's Lester Newman Undergraduate Research Scholars Program and Spike Wadsworth and Y. Sherry Sheng Fund for Biology, both programmes at Portland State University

LITERATURE CITED

Aellen, V. (1952). Contribution à l'étude des chiroptères du Cameroun. *Mémoires de la Société Neuchâteloise des Sciences Naturelles*, *8*, 1–121.

Amori, G., Segniagbeto, G. H., Decher, J., Assou, D., Gippoliti, S., & Luiselli, L. (2016). Non-marine mammals of Togo (West Africa): an annotated checklist. *Zoosystema*, *38*, 201–244. https://doi.org/10.5252/z2016n2a3

Awa, T., II, Dzikouk, G., & Norris, K. (2009). Breeding distribution and population decline of globally threatened Grey-necked Picathartes *Picathartes oreas* in Mbam Minkom Mountain Forest, southern Cameroon. *Bird Conservation International*, *19*, 254–264. https://doi.org/10.1017/S0959270909008363

Bakwo Fils, E. M. (2010). The Bats of Cameroon: Proving the Benefits of Forgotten Fruit Bats. *BATS*, *28*, 11–13.

Bakwo Fils, E. M., Anong, A. G. B. A., Tsala, D. B., Guieké, B. B., Tsala, D. E., & Fotso, A. K. (2014). Diversity of bats of the Far North Region of Cameroon–with two first records for the country. *Biodiversity*, *15*, 16–22. https://doi.org/10.1080/14888386.2014.889578

Bickham, J. W., Patton, J. C., Schlitter, D. A., Rautenbach, I. L., & Honeycutt, R. L. (2004). Molecular phylogenetics, karyotypic diversity, and partition of the genus Myotis (Chiroptera: Vespertilionidae). *Molecular Phylogenetics and Evolution*, *33*, 333–338.

Bickham, J. W., Wood, C. C., & Patton, J. C. (1995). Biogeographic implications of cytochrome b sequences and allozymes in sockeye (*Oncorhynchus nerka*). *The Journal of Heredity*, *86*, 140–144.

Bissaya, R., Ghogomu, R. T., Akissebini, S. M., Njom, B., Gomssi, E. L., & Kanouo, N. S. (2018). Geomorphological approach in active tectonics for the cartography of landslide and rock fall hazards in the North-West part of the region of Yaounde-Cameroon. *The International Journal of Engineering and Science*, *7*, 73–96.

Booth, A. H. (1954). The Dahomey Gap and the mammalian fauna of the West African forests. *Revue de Zoologie et de Botanique Africaines*, *50*, 305–314.

Booth, A. H. (1958). The Niger, the Volta and the Dahomey Gap as geographic barriers. *Evolution*, *12*, 48–62.

Borgelt, J., Dorber, M., Høiberg, M. A., & Verones, F. (2022). More than half of data deficient species predicted to be threatened by extinction. *Communications Biology*, *5*, 679. https://doi.org/10.1038/s42003-022-03638-9

Caetano, G. H., de, O., Chapple, D. G., Grenyer, R., Raz, T., Rosenblatt, J., Tingley, R., Böhm, M., Meiri, S., & Roll, U. (2022). Automated assessment reveals that the extinction risk of reptiles is widely underestimated across space and phylogeny. *PLoS Biology*, *20*, e3001544. https://doi.org/10.1371/journal.pbio.3001544

Carcasson, R. H. (1964). A preliminary survey of the zoogeography of African butterflies. *African Journal of Ecology*, *2*, 122–157. https://doi.org/10.1111/j.1365-2028.1964.tb00203.x

Copernicus Sentinel data. (2022). Retrieved from ASF DAAC [27 May 2022], processed by ESA.

Darriba, D., Taboada, G. L., Doallo, R., & Posada, D. (2012). jModelTest 2: more models, new heuristics and parallel computing. *Nature Methods*, *9*, 772–772. https://doi.org/10.1038/nmeth.2109

Day, R. W., & Quinn, G. P. (1989). Comparisons of treatments after an analysis of variance in ecology. *Ecological Monographs*, *59*, 433–463. https://doi.org/10.2307/1943075

Decher, J., Hoffmann, A., Schaer, J., Norris, R. W., Kadjo, B., Astrin, J., Monadjem, A., & Hutterer, R. (2015). Bat diversity in the Simandou Mountain Range of Guinea, with the description of a new white-winged vespertilionid. *Acta Chiropterologica*, *17*, 255–282. https://doi.org/10.3161/15081109ACC2015.17.2.003

Demenou, B. B., Doucet, J. L., & Hardy, O. J. (2018). History of the fragmentation of the African rain forest in the Dahomey Gap: insight from the demographic history of *Terminalia superba*. *Heredity*, *120*, 547–561. https://doi.org/10.1038/s41437-017-0035-0

Demenou, B. B., Piñeiro, R., & Hardy, O. J. (2016). Origin and history of the Dahomey Gap separating West and Central African rain forests: insights from the phylogeography of the legume tree *Distemonanthus benthamianus*. *Journal of Biogeography*, *43*, 1020–1031. https://doi.org/10.1111/jbi.12688

Demos, T. C., Webala, P. W., Goodman, S. M., Kerbis Peterhans, J. C., Bartonjo, M., & Patterson, B. D. (2019). Molecular phylogenetics of the African horseshoe bats (Chiroptera: Rhinolophidae): expanded geographic and taxonomic sampling of the Afrotropics. *BMC Evolutionary Biology*, *19*, 1–14. https://doi.org/10.1186/s12862-019-1485-1

Demos, T. C., Webala, P. W., Lutz, H. L., Kerbis Peterhans, J. C., Goodman, S. M., Cortés-Delgado, N., Bartonjo, M., & Patterson, B. D. (2020). Multilocus phylogeny of a cryptic radiation of Afrotropical long-fingered bats (Chiroptera, Miniopteridae). *Zoologica Scripta*, *49*, 1–13. https://doi.org/10.1111/zsc.12388

Denys, C., Missoup, A. D., Nicolas, V., Fülling, O., Delapré, A., Bilong, C. F. B., Taylor, P. J., & Hutterer, R. (2014). African highlands as mammal diversity hotspots: new records of *Lamottemys okuensis* Petter, 1986 (Rodentia: Muridae) and other endemic rodents from Mt Oku, Cameroon. *Zoosystema*, *36*, 647–690. https://doi.org/10.5252/z2014n3a6

Dongmo, E. M., Bakwo Fils, E.-M., Manga Mongombe, A., & Tchuenguem Fohouo, F.-N. (2020). Diversity of bats (Mammalia: Chiroptera) along an altitudinal gradient in the western region of Cameroon. *Bonn Zoological Bulletin*, *69*, 45–54.

Edgar, R. C. (2004). MUSCLE: multiple sequence alignment with high accuracy and high throughput. *Nucleic Acids Research*, *32*, 1792–1797. https://doi.org/10.1093/nar/gkh340

Eisentraut, M. (1941). Beitrag zur Oekologie Kameruner Chiropteren. *Mitteilungen Aus Dem Zoologischen Museum in Berlin*, *25*, 245–273.

Eisentraut, M. (1956). Beitrag zur Chiropteren-Fauna von Kamerun (Westafrika). *Zoologische Jahrbücher: Abteilung Für Systematik*, *84*, 505–540.

Eisentraut, M. (1957). Beitrag zur Säugetierfauna des Kamerungebirges und Verbreitung der Arten in den verschiedenen Höhenstufen. *Zoologische Jahrbücher: Abteilung Für Systematik*, *85*, 619–672.

Eisentraut, M. (1963). *Die Wirbeltiere des Kamerungebirges. Unter besonderer Berücksichtigung des Faunenwechsels in den verschiedenen Höhenstufen*. P Parey.

Eisentraut, M. (1973). Die Wirbelthierefauna von Fernando Poo und Westkamerun, Unter besonderer Berücksichtigung der Bedeutung der pleistozänen Klimaschwankungen für die heutige Faunenverteilung. *Bonner Zoologische Monographien*, *3*, 1–428.

Esri Inc. (2020). *ArcGIS Pro* (Version 2.5). Esri Inc. https://www.esri.com/en-us/arcgis/products/arcgis-pro/overview.

Fedden, M. O., & MacLeod, H. L. (1986). Bat research in western Cameroon. In S. N. Stuart (Ed.), *Conservation of Cameroon Montane Forest: Report of the ICBP Cameroon Montane Forest Survey November 1983-April 1984* (pp. 175–195). International Council for Bird Preservation.

Ferreira, D. F., Jarrett, C., Atagana, P. J., Powell, L. L., & Rebelo, H. (2021). Are bat mist nets ideal for capturing bats? From ultrathin to bird nets, a field test. *Journal of Mammalogy*, *102*, 1627–1634. https://doi.org/10.1093/jmammal/gyab109

Flaquer, C., Torre, I., & Arrizabalaga, A. (2007). Comparison of sampling methods for inventory of bat communities. *Journal of Mammalogy*, *88*, 526–533. https://doi.org/10.1644/06-MAMM-A-135R1.1

Gray, J. E. (1821). On the natural arrangement of vertebrose animals. *London Medical Repository*, *15*, 296–310.

Grubb, P. (1978). Patterns of speciation in African mammals. *Bulletin of the Carnegie Museum of Natural History*, *6*, 152–167.

Hall, E. R., & Russell, W. C. (1933). Dermestid beetles as an aid in cleaning bones. *Journal of Mammalogy*, *14*, 372–374. https://doi.org/10.1093/jmammal/14.4.372

Happold, M., & Happold, D. (Ed.). (2013). *Mammals of Africa: Vol. IV, Hedgehogs, Shrews and Bats*. Bloomsbury Publishing.

Herkt, K. M. B., Barnikel, G., Skidmore, A. K., & Fahr, J. (2016). A high-resolution model of bat diversity and endemism for continental. *Africa. Ecological Modeling*, *320*, 9–28. https://doi.org/10.1016/j.ecolmodel.2015.09.009

Hutterer, R., Decher, J., Monadjem, A., & Astrin, J. (2019). A new genus and species of vesper bat from West Africa, with notes on *Hypsugo*, *Neoromicia*, and *Pipistrellus* (Chiroptera: Vespertilionidae). *Acta Chiropterologica*, *21*, 1–22. https://doi.org/10.3161/15081109ACC2019.21.1.001

IUCN [International Union for the Conservation of Nature]. (2021). *The IUCN Red List of Threatened Species*. May 24, 2021. https://www.iucnredlist.org

Juste, J., Torrent, L., Méndez-Rodríguez, A., Howard, K., García-Mudarra, J. L., Nogueras, J., & Ibáñez, C. (2023). A new Pipistrelle bat from the oceanic Island of Príncipe (Western Central Africa). *Journal of Mammalogy*, *104*, in press.

Kumar, S., Stecher, G., Li, M., Knyaz, C., & Tamura, K. (2018). MEGA X: molecular evolutionary genetics analysis across computing platforms. *Molecular Biology and Evolution*, *35*, 1547–1549. https://doi.org/10.1093/molbev/msy096

Lebreton, M., Bakwo Fils, E. M., Takuo, J. M., & Le Doux Diffo, J. (2014). The first record of the African Sheath-tailed Bat *Coleura afra* (Peters, 1852) (Mammalia, Chiroptera) in Cameroon with information on its ecology. *African Bat Conservation News*, *36*, 2–4.

Linder, H. P., de Klerk, H. M., Born, J., Burgess, N. D., Fjeldså, J., & Rahbek, C. (2012). The partitioning of Africa: statistically defined biogeographical regions in sub–Saharan Africa. *Journal of Biogeography*, *39*, 1189–1205. https://doi.org/10.1111/j.1365-2699.2012.02728.x

Livingstone, D. A. (1975). Late Quaternary climatic change in Africa. *Annual Review of Ecology and Systematics*, *6*, 249–280. https://doi.org/10.1146/annurev.es.06.110175.001341

Lönnberg, E. (1929). The development and distribution of the African fauna in connection with and depending upon climatic changes. *Arkiv för zoologi*, *21A*, 1–33.

Manga Mongombe, A., Bakwo Fils, E. M., & Tamesse, J. L. (2019). Diversity and altitudinal distribution of bats (Mammalia: Chiroptera) on Mount Cameroon. *Tropical Zoology*, *32*, 166–187. https://doi.org/10.1080/03946975.2019.1680077

Miller, M. A., Pfeiffer, W., & Schwartz, T. (2010, November 14) *Creating the CIPRES Science Gateway for inference of large phylogenetic trees* [Paper presentation]. 2010 Gateway Computing Environments Workshop (GCE), pp. 1–8, https://doi.org/10.1109/GCE.2010.5676129

Monadjem, A., Demos, T. C., Dalton, D. L., Webala, P. W., Musila, S., Kerbis Peterhans, J. C., & Patterson, B. D. (2021). A revision of pipistrelle-like bats (Mammalia: Chiroptera: Vespertilionidae) in East Africa with the description of new genera and species. *Zoological Journal of the Linnean Society*, *191*, 1114–1146. https://doi.org/10.1093/zoolinnean/zlaa087

Monadjem, A., Richards, L. R., Decher, J., Hutterer, R., Mamba, M. L., Guyton, J., Naskrecki, P., Markotter, W., Wipfler, B., Kropff, A. S., & Dalton, D. L. (2021). A phylogeny for African *Pipistrellus* species with the description of a new species from West Africa (Mammalia: Chiroptera). *Zoological Journal of the Linnean Society*, *191*, 1114–1146. https://doi.org/10.1093/zoolinnean/zlaa068

Monadjem, A., Richards, L., & Denys, C. (2016). An African bat hotspot: the exceptional importance of Mount Nimba for bat diversity. *Acta Chiropterologica*, *18*, 359–375. https://doi.org/10.3161/15081109ACC2016.18.2.005

Monadjem, A., Richards, L., Taylor, P. J., & Stoffberg, S. (2013). High diversity of pipistrelloid bats (Vespertilionidae: *Hypsugo*, *Neoromicia*, and *Pipistrellus*) in a West African rainforest with the description of a new species. *Zoological Journal of the Linnean Society*, *167*, 191–207. https://doi.org/10.1111/j.1096-3642.2012.00871.x

Monadjem, A., Shapiro, J. T., Richards, L. R., Karabulut, H., Crawley, W., Nielsen, I. B., Hansen, A., Bohmann, K., & Mourier, T. (2020). Systematics of West African *Miniopterus* with the description of a new species. *Acta Chiropterologica*, *21*, 237–256. https://doi.org/10.3161/15081109ACC2019.21.2.001

Moreau, R. E. (1952). Africa since the Mesozoic: with particular reference to certain biological problems. *Proceedings of the Zoological Society of London*, *121*, 869–913. https://doi.org/10.1111/j.1096-3642.1952.tb00789.x

Moreau, R. E. (1963). Vicissitudes of the African biomes in the late Pleistocene. *Proceedings of the Zoological Society of London*, *141*, 395–421. https://doi.org/10.1111/j.1469-7998.1963.tb01618.x

Moreau, R. E. (1966). *The bird faunas of Africa and its islands*. Academic Press.

Moreau, R. E. (1969). Climatic changes and the distribution of forest vertebrates in West Africa. *Journal of Zoology*, *158*, 39–61. https://doi.org/10.1111/j.1469-7998.1969.tb04965.x

Nguyen, L. T., Schmidt, H. A., Von Haeseler, A., & Minh, B. Q. (2015). IQ-TREE: a fast and effective stochastic algorithm for estimating maximum-likelihood phylogenies. *Molecular Biology and Evolution*, *32*, 268–274. https://doi.org/10.1093/molbev/msu300

Oksanen, J., Blanchet, F. G., Friendly, M., Kindt, R., Legendre, P., McGlinn, D., Minchin, P. R., O'Hara, R. B., Simpson, G. L., Solymos, P., Stevens, M. H. H., Szoecs, E., Wagner, H. (2020). *Vegan: community ecology package*. R package version 4.2.0. http://cran.r-project.org

Olson, D. M., Dinerstein, E., Wikramanayake, E. D., Burgess, N. D., Powell, G. V. N., Underwood, E. C., D'amico, J. A., Itoua, I., Strand, H. E., Morrison, J. C., Loucks, C. J., Allnutt, T. F., Ricketts, T. H., Kura, Y., Lamoreux, J. F., Wettengel, W. W., Hedao, P., & Kassem, K. R. (2001). Terrestrial Ecoregions of the World: A New Map of Life on Earth. *BioScience*, *51*, 933–938. https://doi.org/10.1641/0006-3568(2001)051[0933:TEOTWA2.0.CO;2]

Pahl, A. (2020). Skeleton preparation best practices in the modern museum: the dermestid approach. *Curator: The Museum Journal*, *63*, 99–113. https://doi.org/10.1111/cura.12349

Patterson, B. D., Webala, P. W., Rossoni, D., & Demos, T. C. (2021, June 14–18) *Diversification histories of Afrotropical bats: lessons from 21 genera* [Paper presentation, no. 363]. 100th Annual Meeting of the American Society of Mammalogists (online at: https://asm.econference.io/public/hqHFK3h/main/sessions/955), held virtually.

Perret, J. L., & Aellen, V. (1956). Mammifères du Cameroun de la collection J. L. Perret. *Revue Suisse de Zoologie*, *63*, 395–450. https://doi.org/10.5962/bhl.part.75468

Peters, W. C. H. (1852). *Naturwissenschaftliche Reise nach Mossambique, auf Befehl Seiner Majestät des Königs Friedrich Wilhelm IV, in den Jahren 1842 bis 1848 ausgeführt, von Wilhelm C. H. Peters. Zoologie*. Georg Reimer.

Peters, W. (1872). Eine Mittheilung über neue Flederthiere (*Phyllorhina micropus, Harpyiocephalus Huttoni, Murina grisea, Vesperugo micropus, Vesperus (Marsipolæmus) albigularis, Vesperus propinquus, tenuipinnis*). *Monatsberichte de Könniglichen Preussische Akademie des Wissenschaften zu Berlin, 1872*, 256–264.

R Core Team. (2020). *R: a language and environment for statistical computing (Version 4.2.0) [Computer software]*. R Foundation for Statistical Computing. https://www.R-project.org/

Rambaut, A., Drummond, A. J., Xie, D., Baele, G., & Suchard, M. A. (2018). Posterior summarization in Bayesian phylogenetics using Tracer 1.7. *Systematic Biology*, *67*, 901–904. https://doi.org/10.1093/sysbio/syy032

Robbins, C. B. (1978). The Dahomey Gap – a reevaluation of its significance as a faunal barrier to west African high forest mammals. *Bulletin of the Carnegie Museum of Natural History*, *6*, 168–174.

Ronquist, F., Teslenko, M., van der Mark, P., Ayres, D. L., Darling, A., Höhna, S., Larget, B., Liu, L., Suchard, M. A., & Huelsenbeck, J. P. (2012). MrBayes 3.2: efficient Bayesian phylogenetic inference and model choice across a large model space. *Systematic Biology*, *61*, 539–542. https://doi.org/10.1093/sysbio/sys029

Rowan, J., Kamilar, J. M., Beaudrot, L., & Reed, K. E. (2016). Strong influence of palaeoclimate on the structure of modern African mammal communities. *Proceedings of the Royal Society B: Biological Sciences*, *283*, 20161207. https://doi.org/10.1098/rspb.2016.1207

Ruedas, L. A. (1998). Systematics of *Sylvilagus* Gray, 1867 (Lagomorpha: Leporidae) from southwestern North America. *Journal of Mammalogy*, *79*, 1355–1378. https://doi.org/10.2307/1383027

Russell, W. C. (1947). Biology of the dermestid beetle with reference to skull cleaning. *Journal of Mammalogy*, *28*, 284–287.

SAS Institute Inc. (2018). *SAS/STAT® 15.1 User's Guide*. SAS Institute Inc.

Sikes, R. S, and the Animal Care and Use Committee of the American Society of Mammalogists. (2016). 2016 Guidelines of the American Society of Mammalogists for the use of wild mammals in research and education. *Journal of Mammalogy*, *97*, 663–688. https://doi.org/10.1093/jmammal/gyw078

Simo, M., Droissart, V., Sonké, B., & Stevart, T. (2009). The orchid flora of the Mbam Minkom hills (Yaoundé, Cameroon). *Belgian Journal of Botany*, *142*, 111–123.

Smithe, F. B. (1974). *Naturalist's color guide supplement*. The American Museum of Natural History.

Tanshi, I., Obitte, B. C., Monadjem, A., & Kingston, T. (2022a). Hidden Afrotropical bat diversity in Nigeria: ten new country records from a biodiversity hotspot. *Acta Chiropterologica*, *23*, 313–343. https://doi.org/10.3161/15081109ACC2021.23.2.004

Tanshi, I., Obitte, B. C., Monadjem, A., Rossiter, S. J., Fisher-Phelps, M., & Kingston, T. (2022b). Multiple dimensions of biodiversity in paleotropical hotspots reveal comparable bat diversity. *Biotropica*, *54*, 1205–1216. https://doi.org/10.1111/btp.13143

Thomas, O. (1880). On bats from Old Calabar. *Annals and Magazine of Natural History, Series 5*, *6*, 164–167. https://doi.org/10.1080/00222938009458914

Thomas, O. (1889). Description of a new bat from the Gambia. *Annals and Magazine of Natural History, Series 6*, *3*, 362–364. https://doi.org/10.1080/00222938909460347

Van Cakenberghe, V. & Seamark, E. C. J. (Eds.). (2021). *African Chiroptera Report 2021*. AfricanBats NPC.

Van Cakenberghe, V., & Happold, M. (2013). *Pipistrellus rendalli,* Rendall's Pipistrelle. In M. Happold & D. Happold, (Eds.), *Mammals of Africa. Volume IV. Hedgehogs, shrews and bats* (pp. 645–647). Bloomsbury Publishing.

Velazco, P. M., & Gardner, A. L. (2012). A new species of *Lophostoma* d'Orbigny, 1836 (Chiroptera: Phyllostomidae) from Panama. *Journal of Mammalogy*, *93*, 605–614. https://doi.org/10.1644/11-MAMM-A-217.1

Voss, R. S., Marcus, L. F., & Escalante, P. P. (1990). Morphological evolution in muroid rodents I. Conservative patterns of craniometric covariance and their ontogenetic basis in the Neotropical genus *Zygodontomys*. *Evolution; International Journal of Organic Evolution*, *44*, 1568–1587. https://doi.org/10.2307/2409338

Waghiiwimbom, M. D., Bakwo Fils, E. M., Atagana, P. J., Tsague Kenfack, J. A., & Tamesse, J. L. (2020). Diversity and community structure of bats (Chiroptera) in the Centre Region of Cameroon. *African Journal of Ecology*, *58*, 211–226. https://doi.org/10.1111/aje.12692

White, F. (1983). *The vegetation of Africa. A descriptive memoir to accompany the Unesco/AETFAT/UNSO vegetation map of Africa*. United Nations Educational, Scientific and Cultural Organization.

Wickham, H. (2016). *ggplot2: Elegant Graphics for Data Analysis*. Springer-Verlag. https://ggplot2.tidyverse.org.

Wilcoxon, F. (1945). Individual comparisons by ranking methods. *Biometrics Bulletin*, *1*, 80–83. https://doi.org/10.2307/3001968